



LJMU Research Online

Dulaimi, A, Al Busaltan, S, Mydin, MAO, Lu, D, Özkılıç, YO, Jaya, RP and Ameen, A

Innovative geopolymer-based cold asphalt emulsion mixture as eco-friendly material

<http://researchonline.ljmu.ac.uk/id/eprint/22744/>

Article

Citation (please note it is advisable to refer to the publisher's version if you intend to cite from this work)

Dulaimi, A, Al Busaltan, S, Mydin, MAO, Lu, D, Özkılıç, YO, Jaya, RP and Ameen, A (2023) Innovative geopolymer-based cold asphalt emulsion mixture as eco-friendly material. Scientific Reports, 13 (1). pp. 1-14. ISSN 2045-2322

LJMU has developed [LJMU Research Online](#) for users to access the research output of the University more effectively. Copyright © and Moral Rights for the papers on this site are retained by the individual authors and/or other copyright owners. Users may download and/or print one copy of any article(s) in LJMU Research Online to facilitate their private study or for non-commercial research. You may not engage in further distribution of the material or use it for any profit-making activities or any commercial gain.

The version presented here may differ from the published version or from the version of the record. Please see the repository URL above for details on accessing the published version and note that access may require a subscription.

For more information please contact researchonline@ljmu.ac.uk

<http://researchonline.ljmu.ac.uk/>



OPEN Innovative geopolymer-based cold asphalt emulsion mixture as eco-friendly material

Anmar Dulaimi^{1,2,3✉}, Shakir Al Busaltan³, Md Azree Othuman Mydin⁴, Dong Lu^{5,6}, Yasin Onuralp Özkılıç^{7,8}, Ramadhansyah Putra Jaya⁹ & Arman Ameen^{10✉}

In recent years, there has been a growing interest in cold asphalt emulsion mixture (CAEM) due to its numerous advantages, including reduced CO₂ emissions, energy savings, and improved safety during construction and application. However, CAEM has often been considered inferior to hot mix asphalt (HMA) in terms of performance. To address this issue and achieve desirable performance characteristics, researchers have been exploring the modification of CAEM using high-cost additives like ordinary Portland cement. In this study, the focus was on investigating the effects of utilizing waste alkaline Ca(OH)₂ solution, ground granulated blast-furnace slag (GGBFS), and calcium carbide residue (CCR) as modifiers to enhance the properties of CAEM. The aim was to develop an innovative geopolymer geopolymer-based cold asphalt emulsion mixture (GCAE). The results of the study revealed that the use of waste alkaline Ca(OH)₂ solution led to an increase in early hydration, which was confirmed through scanning electron microscopy. Furthermore, the experimental findings demonstrated that waste alkaline Ca(OH)₂ solution significantly contributed to the rapid development of early-age strength in GCAE. As a result, GCAE showed great potential for utilization in pavement applications, particularly for roads subjected to harsh service conditions involving moisture and temperature. By exploring these alternative modifiers, the study highlights a promising avenue for enhancing the performance of CAEM and potentially reducing the reliance on expensive additives like ordinary Portland cement. The development of GCAE has the potential to offer improved performance and durability in pavement applications, thus contributing to sustainable and efficient road infrastructure.

Abbreviations

CAEM	Cold asphalt emulsion mixture
CBEM	Cold bitumen emulsion mixture
CCR	Calcium carbide residue
CMA	Cold mix asphalt
EACM	Emulsified asphalt cold mix
GCAE	Geopolymer geopolymer-based cold asphalt emulsion mixture
GGBFS	Ground granulated blast-furnace slag
HMA	Hot mix asphalt
ITSM	Indirect tensile stiffness modulus test
LF	Limestone filler
OPC	Ordinary Portland cement

¹College of Engineering, University of Warith Al-Anbiyaa, Karbala 56001, Iraq. ²School of Civil Engineering and Built Environment, Liverpool John Moores University, Liverpool L3 2ET, UK. ³Department of Civil Engineering, College of Engineering, University of Kerbala, Karbala 56001, Iraq. ⁴School of Housing, Building and Planning, Universiti Sains Malaysia, 11800 Penang, Malaysia. ⁵School of Civil Engineering, Harbin Institute of Technology, Harbin 150090, People's Republic of China. ⁶Key Lab of Structures Dynamic Behavior and Control of the Ministry of Education, Harbin Institute of Technology, Harbin 150090, People's Republic of China. ⁷Department of Civil Engineering, Faculty of Engineering, Necmettin Erbakan University, 42000 Konya, Turkey. ⁸Department of Civil Engineering, Lebanese American University, Byblos 1102-2801, Lebanon. ⁹Faculty of Civil Engineering Technology, Universiti Malaysia Pahang Al-Sultan Abdullah, 26300 Kuantan, Malaysia. ¹⁰Department of Building Engineering, Energy Systems and Sustainability Science, University of Gävle, 801 76 Gävle, Sweden. ✉email: a.f.dulaimi@uowa.edu.iq; a.f.dulaimi@ljamu.ac.uk; arman.ameen@hig.se

SCB	Semi-circular bending
SCM	Secondary cementitious material
SEM	Scanning electron microscopy
SMR	Stiffness modulus ratio
TLF	Traditional limestone filler
WMA	Warm mix asphalt
XRD	X-ray diffraction
XRF	X-ray fluorescence technique

Global warming stands as one of the most critical challenges we face today, and the construction industry plays a significant role in contributing to greenhouse gas emissions. In response to this issue, various sectors are adopting sustainable practices and products, and the highway industry is actively taking steps to minimize its carbon footprint. While hot mix asphalt (HMA) remains widely utilized for pavement construction due to its lower initial cost and superior performance^{1,2}, it is produced at high temperatures (> 140 °C), leading to adverse environmental impacts such as the release of greenhouse gases and hazardous fumes^{3–5}.

Cold asphalt emulsion mixture (CAEM) refers to a type of cold mix asphalt (CMA) that is produced by combining emulsified bitumen with unheated aggregates. This method eliminates the need for aggregate heating, making CAEM cost-effective and environmentally friendly^{6,7}. Although CMA offers advantages in terms of cost and environmental impact compared to warm mix asphalt (WMA) and hot mix asphalt (HMA), it falls short in terms of strength and stability. The Marshall Stability values of unmodified CMA are significantly lower than those of HMA and WMA^{8,9}. Additionally, CMA tends to have higher air voids compared to HMA, which can impact its service life negatively¹⁰. As a result, CMA is typically used for footpath reinstatement and low-to-moderate-traffic roadways^{11–15}.

Numerous studies have been carried out to see how different types of filler materials affect CMA performance. Filler materials, typically those that pass through a sieve size of 75 µm, are commonly used in asphalt mixes. Furthermore, Ordinary Portland Cement (OPC) has been extensively employed as a hydraulic binder to produce CAEMs that exhibit satisfactory performance^{16,17}. The cement-modified CMA has increased strength and resistance to water damage, temperature sensitivity, permanent deformation and creep^{18,19}. Wang et al.²⁰ demonstrated that the cement paste has alkaline nature, so the breakdown of the cationic bitumen emulsion can be accelerated by raising the pH due to the presence of OPC in the CMA. This allows the flocculation of the asphalt emulsion and makes a rapid coalescence due to the increase in the dissociation rate of the emulsifier on the asphalt droplets. However, the manufacture of one ton of OPC emits about one ton of carbon dioxide and consumes roughly 2.5 tonnes of materials²¹, accounting for about 7% of total greenhouse gas emissions worldwide²². As a result, reports of the manufacture of CAEMs using industrial by-products or solid wastes began to circulate^{23,24}.

Industrial by-products and solid waste are becoming a growing concern worldwide, leading to significant environmental and economic challenges. To address this issue, there is an increasing trend in developing cold asphalt emulsion mixture (CAEM) using different by-products and waste materials. One such by-product is ground granulated blast-furnace slag (GGBFS), which is obtained through the grinding of blast-furnace slag, a residue of the iron-making industry. For many years, GGBFS has been widely utilized in Portland cement concrete as a secondary cementitious material (SCM), either as a mineral additive or as a component of blended cement, often replacing 35–65% of ordinary Portland cement (OPC)²⁵. It was demonstrated by Ellis et al.²⁶ that in comparison to reference mixes, adding GGBFS to CAEM mixes increased long-term mechanical performance. In addition, comparison research was carried out with two types of fillers, namely cement and GGBFS (each of 2% by the total mass of the mix), and performance was measured in terms of Marshall characteristics²⁷. However, the GGBFS had a greater Marshall Stability, the cement had a higher density and fewer air voids. The inclusion of a low cement percentage (1%) in combination with ground granulated blast-furnace slag (GGBFS) and fly ash has been shown to enhance the mechanical properties and durability of cold mix asphalt (CMA), resulting in performance comparable to high cement content HMA and CMA²⁸. Bijen²⁹ also found that GGBFS, with its high lime content, acts as a latent hydraulic cement that requires activation. Since GGBFS exhibits a slower hydration rate compared to Portland cement, activators for example alkalis, Portland cement, or lime are used to accelerate the process³⁰.

Calcium carbide residue (CCR) is a waste product generated during the hydrolysis of calcium carbide to produce acetylene gas. Due to its high alkalinity and significant metal content, CCR seriously harms the environment³¹. The high alkalinity of CCR makes it appropriate for activating GGBFS, thereby enhancing its reactivity during the early stages^{32,33}.

On the other hand, because geopolymers have environmentally friendly features, they can partially or completely replace OPC, and their solid precursors include fly ash, metakaolin, slag, and other materials^{34–36}.

Geopolymers have been attracting the attention of researchers due to their feasibility, low cost, and environmentally friendly nature, making them viable alternatives to organic polymers in road construction³⁷. The strength development of recycled asphalt pavement using fly ash geopolymers has been studied as a potential road construction material. Hoy et al.³⁸ further confirm the potential of these geopolymers as alternative stabilized pavement materials in their research work. The incorporation of recycled asphaltic concrete aggregate can be advantageous in enhancing the performance of geopolymer concrete. Despite a minor reduction in compressive strength, it offers improved resistance against surface abrasion and sulfuric acid. By enhancing sulfuric acid resistance and surface abrasion while maintaining reasonable compressive strength, the use of recycled asphaltic concrete aggregate becomes beneficial in improving the overall performance of geopolymer concrete³⁹. Meng et al.⁴⁰ investigated the microscopic and mechanical properties of geopolymer-modified asphalt binders and asphalt mixtures. The geopolymer was produced by using alkali activators and aluminosilicate components,

which were then employed as asphalt modifiers. Their findings demonstrate that, with the exception of ductility, the modified binders' fundamental characteristics and high-temperature performance improved. It was also reported that geopolymer has been shown to be a promising ingredient for creating warm mix asphalt with excellent performance and significant advantages where the optimal dose of geopolymer additive by weight of bitumen was 6%, while the optimum mixing temperature for warm mix asphalt was around 140 °C⁴¹. It was found that crushed rock-based alkaline-activated materials, with an optimized mixture comprising a 5 M NaOH concentration, an SS/SH ratio of 1.00, and a liquid alkaline-to-binder (L/B) ratio of 0.5, showed potential for use in roadway applications. Paste samples, cured at room temperature, exhibited an early compressive strength of 3.82 MPa at 3 days of age⁴². Previous study showed that non-OPC binder, based on a hybrid material concept, holds significant potential as an environmentally friendly choice for road construction and rehabilitation in the emerging era of our low-carbon society⁴³.

The traditional CMA, characterized by modest early-age strength performance and inadequate water stability, poses practical limitations in meeting the requirements of rapid open traffic, particularly from an engineering performance standpoint. The objective of this study is to present a new approach for developing CAEM using the geopolymer technique as a sustainable pavement material. To investigate the strength development of CAEM geopolymer, a series of extensive laboratory experiments were conducted.

The use of CAEM with GGBFS-CCR based geopolymer by incorporating waste Ca(OH)₂ solution, a sustainable alternative to HMA, in road pavement has a substantial influence on pavement applications. The durability and mechanical performance of CAEM have been greatly enhanced by the application of various additives, such as OPC. However, such additives could come at a higher starting cost and even increase transportation costs. Additionally, GGBFS, CCR and waste Ca(OH)₂ solution are produced as waste material, creating environmental and health risks. The large quantities of waste produced pose significant challenges in terms of disposal and create engineering hurdles for their utilization in civil construction. As a consequence, there has been a growing interest in incorporating these waste materials in the development of a novel CAEM.

Materials and method

Aggregate

According to BS EN 933-1⁴⁴, a close-graded, surface coarse gradation of 14 mm was selected, which complied with BS EN standards (Fig. 1). This particular gradation is widely used for producing bituminous mixes⁴⁵. The coarse aggregates used in both the CAEMs and HMA consist of crushed granite with the following properties: water absorption of 0.7%, bulk particle density of 2.60 Mg/m³, and apparent particle density of 2.65 Mg/m³. On the other hand, the fine aggregate possesses water absorption of 1.5%, a bulk particle density of 2.53 Mg/m³, and an apparent particle density of 2.64 Mg/m³.

Bitumen emulsion and asphalt

At room temperature, the emulsion has a decreased viscosity, making it a good CAEMs binding material. For all of the CAEMs, a cationic, slow-setting bitumen emulsion (C50B4) was chosen as the binder. This bitumen emulsion has a penetration grade of 40/60 and is made up of 50% base bitumen and supplied by Jobling Purser of Newcastle, UK.

asphalt

Two HMAs were included in this study for comparison purposes. These mixtures have the same aggregate type and grade as the CAEMs. The soft grade penetration (142 pen) has softening point and density (at 25 °C) of 51.5 °C and 1.02 g/cm³, while hard grade penetration (49 pen) has softening point and density (at 25 °C) of 43.5 °C and 1.04 g/cm³, respectively. 5.1% optimum binder content by aggregate weight was used in this study.

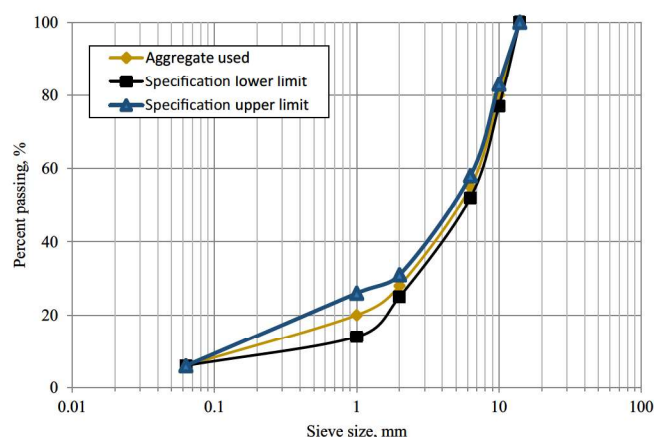


Figure 1. AC 14 mm Gradation.

Alkaline activator

To increase the pH concentration of the hydration mediums and facilitate the breaking and dissolution of glassy phases in the mixture, a waste $\text{Ca}(\text{OH})_2$ solution with high alkalinity was utilized as an alkaline activator. The pH of this solution, which is discharged from CCR's dewatering process, is 13.8. The 3 percent pre-wetting water content was completely replaced with the waste alkaline $\text{Ca}(\text{OH})_2$ solution.

The advancement of technology in the development of a high-strength cold bitumen emulsion mixture (CBEM) is attributed to the research conducted by Dulaimi et al.⁴⁶. Their study aimed to create a novel CBEM with rapid curing properties. Their findings revealed that by activating a binary blended filler with a waste alkaline NaOH solution, the water susceptibility, mechanical properties, and thermal sensitivity of the CBEM were significantly enhanced.

Selected fillers

In this study, ground granulated blast-furnace slag (GGBFS) and calcium carbide residue (CCR) were selected as fillers, while traditional limestone filler (TLF) was used as a conventional mineral filler. The aim was to investigate and assess the full potential of these materials by examining their key physical, chemical, mineralogical, and morphological characteristics. Calcium carbide residue (CCR) is a by-product of acetylene synthesis, consisting mainly of $\text{Ca}(\text{OH})_2$. It is estimated that approximately 74 g of CCR is produced when 64 g of acetylene is synthesized⁴⁷. CCR is produced as a by-product during the industrial production of acetylene gas. The manufacturing process involves the reaction of calcium carbide (CaC_2) with water, resulting in the formation of acetylene gas (C_2H_2), heat, and lime slurry ($\text{Ca}(\text{OH})_2$). The finished product is a slurry of sludge. The slurry converts into a solid-state residue when the high alkalinity water is fully released, making landfill disposal an expensive and complex task.

In 2014, the global production of acetylene gas reached 500,000 tonnes, resulting in the generation of 1,423,000 tonnes of CCR as waste. It is projected that the production of CCR will continue to increase by 3% until 2020⁴⁸. The CCR was in the form of large, moist bricks that required breaking into smaller pieces and drying in an oven at 110 °C for one day. In order to avoid particle agglomeration, which can have a detrimental effect on the quality of the ground CCR, the resulting lumps underwent additional processing in a mechanical grinder. The grinding process involved low-energy, intense, dry agitation for a duration of 15 min. In the GGBFS powder, the particle size distribution shows that over 90% of the particles are less than 40 μm , whereas the CCR's predominant particle size is practically smaller than 25 μm . When exposed to water, the CCR particles' fineness has a significant impact on how quickly they hydrate. The milling process of the CCR lasted for 15 min, resulting in an average grain size (D50) of 24.6 μm . Figure 2 displays the particle size distribution of the GGBFS, CCR, and TLF, indicating that 90% of the TLF particles were able to pass through an 80 μm sieve. The dominant particle size of the CCR is predominantly below 25 μm , whereas approximately 90% of the GGBFS particles have a size smaller than 40 μm .

A Rigaku Miniflex diffractometer for X-ray diffraction (XRD) was used to conduct the analyses. The samples' diffraction patterns were gathered and subjectively examined throughout a 2θ range from 5° to 60°. The diffraction patterns of the GGBFS, CCR, and TLF are shown in Fig. 3. GGBFS is amorphous and has a halo between 25° and 35° (2θ), whereas CCR is mostly composed of Portlandite and calcite and shows no signs of having any amorphous phases. These alkalis' presence in the CCR will hasten the GGBFS' reactivity. Calcite and quartz make up the TLF's powder XRD pattern.

The main oxides present in CCR were lime and silica, identified using the X-ray fluorescence technique (XRF) with a Shimadzu EDX 720 energy dispersive X-ray fluorescence spectrometer, which aligns with the findings of Hanjitsuwan et al.⁴⁹. On the other hand, a chemical analysis of GGBFS, as depicted in Table 1, revealed the presence of lime, alumina, silica, magnesium, and sodium in its composition. The chemical composition results are in agreement with those examined by Chaunsali and Peethamparan⁵⁰. Because CCR contains a significant amount of calcium oxide, it is appealing for use as a promoter similar to OPC³³. CCR is a possible material for GGBFS activation due to its chemical composition. According to the TLF's chemical compositions, CaO and SiO_2 made up the majority of their composition. Although TLF contains a lot of CaO (77.82%), it is regarded

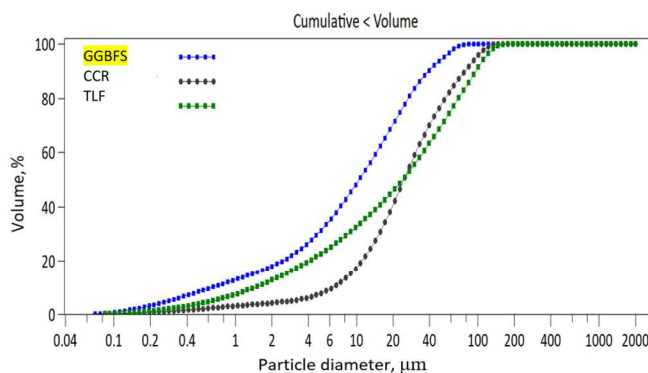


Figure 2. Fillers' particle size distribution.

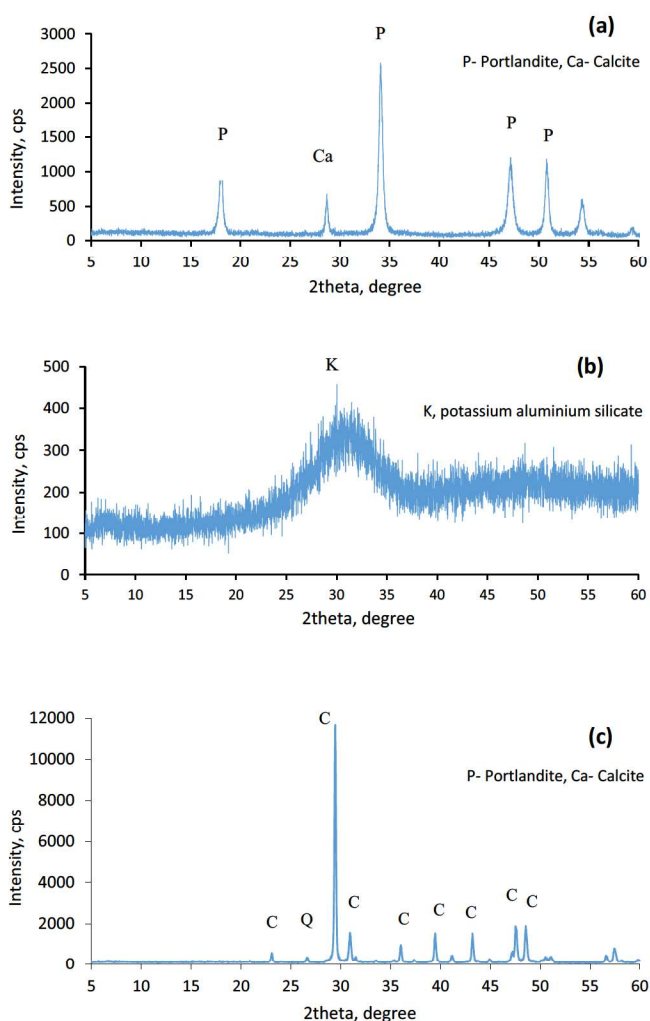


Figure 3. Powder XRD pattern of (a) CCR, b GGBFS and c TLF.

Chemical composition	T LF	GGBFS	CCR
CaO, %	77.82	40.35	81.84
SiO ₂ , %	17.21	37.23	14.08
Al ₂ O ₃ , %	0.0	5.73	0.90
MgO, %	0.89	4.22	0.77
Fe ₂ O ₃ , %	0.0	0.01	0.00
SO ₃ , %	0.01	0.0	0.77
K ₂ O, %	0.35	0.0	0.20
Na ₂ O, %	2.27	0.0	1.32
TiO ₂ , %	0.19	0.63	0.12

Table 1. Comparison of the fillers’ chemical composition.

as an inert substance since CaO doesn’t hydrate when it comes in touch with water because it already exists in a non-hydrated condition.

Figure 4 displays SEM photos of every filler produced by a Quanta 200 using scanning electron microscopy (SEM). Using an auto fine sputter coater, a tiny layer of gold was applied to the samples to improve conductivity. As can be observed, the CCR particles are agglomerated, whereas the GGBFS particles are primarily made up of irregularly shaped particles. This is similar to the study by Hanjitsuwan et al.³³. All TLF particles have sharp angles and rough roughness.

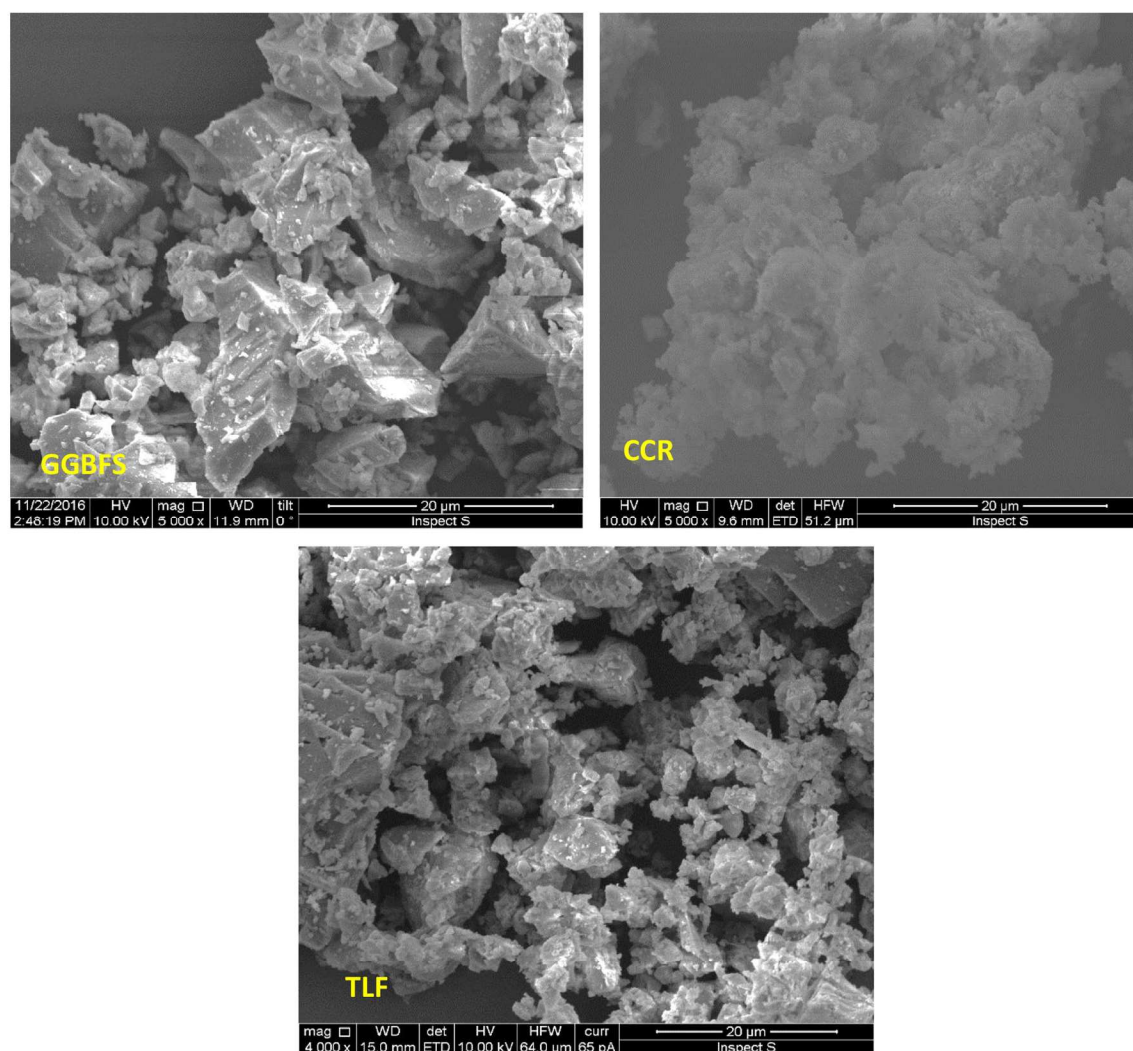


Figure 4. SEM images of the fillers.

The aqueous GGBFS solution had a pH value of 11.6, while the CCR showed a pH of 13.1. This difference in pH levels played a role in the accelerated breakdown of the bitumen emulsion in the CAEMs. On the other hand, the TLF exhibited a pH of 9.39.

Manufacturing of samples

The mix proportions for the CAEMs are shown in Table 2. It was recommended to use 12.5% bitumen emulsion to produce mixes that would increase the CAEMs' early-age strength. Therefore, the fixed amount of 4% GGBFS + 2% CCR was incorporated in accordance with previous research⁵¹. The bitumen emulsion used here with 50% base bitumen, and the pre-wetting water contained was 3%. After that, a 3% waste alkaline $\text{Ca}(\text{OH})_2$ solution replaced the 3% pre-wetting to produce a novel GCAE mix.

In accordance with the recommendations of Dulaimi et al.⁵² and following the Marshall Method for Emulsified Asphalt Aggregate Cold Mixture Design (MS-14)⁵³, the aggregates, including the coarse and fine components, as well as the fillers, were initially mixed with the required pre-wetting water for 1 min at a slow speed to

Mix type	Filler types	Bitumen emulsion, %	Pre-wetting water, %
TLF	6% TLF	12.5%	3%
4GGBFS2CCR	4% GGBFS + 2% CCR	12.5%	3%
GCAE	4% GGBFS + 2% CCR	12.5%	(3%) Alkaline waste $\text{Ca}(\text{OH})_2$ solution
HMA 40/60	6% TLF	5.1% Base binder 40/60	–
HMA 100/150	6% TLF	5.1% Base binder 100/150	–

Table 2. Details on the mix's ratios.

prepare the cold asphalt emulsion mixtures (CAEMs). The bitumen emulsion was gradually added during the subsequent 30 s of mixing. The mixing process continued for an additional 2 min. Afterwards, the mixtures were quickly poured into steel molds and compacted by applying 50 blows with a Marshall hammer to each surface of the samples.

All samples were then extruded using a hydraulic de-moulding jack after being kept in their molds for 24 h. These mixes were compared with both CAEMs (TLF and 4GGBFS2CCR) and conventional hot mix asphalt mixtures.

Laboratory testing programme

This research reports the results of the test of indirect tensile stiffness modulus test (ITSM), wheel truck resistance, water sensitivity and low-temperature cracking susceptibility of a new, novel geopolymer cold asphalt emulsion mixture in addition to the references to traditional CAEMs and HMAs. The procedures for testing emulsified asphalt cold mix (EACM) specimens are shown in Fig. 5.

ITSM test

The ITSM was determined at the standard prescribed ambient temperature of $(20 \pm 1 \text{ }^\circ\text{C})$ as per the following BS EN 12697-26⁵⁴, using a Cooper Research Technology HYD 25 testing machine. Three replicates of each sample were created to evaluate the ITSM. The cylindrical sample was generated by applying 50 blows to each side of the sample, extracting it after 24 h, and storing it in the lab at room temperature for testing over the course of 3, 7, 14, 28 and 56 days. When testing for ITSM, the room temperature was chosen as the standard curing temperature for produced mixes. This procedure was followed to simulate the production, placing, and compacting of CAEMs on the site and to avoid premature binder aging^{53,54}. The Marshall specimens were 101.6 mm in diameter and 63.5 mm in height. The ITSM of the mixes was evaluated using the average of three replicates.

Wheel-tracking test

The assessment of rutting effectiveness was carried out by comparing the performance of GCAE mixes with reference mixes. The evaluation was conducted following European standards outlined in BS EN 12697-22⁵⁵. To measure rut depths, a wheel tracker device of type HYZ-5 was employed. The rutting slab employed in the testing had dimensions of 400 mm \times 305 mm \times 50 mm. The average of three replicates was recorded to evaluate the rutting resistance of the mixes. Before conducting the tests, the slab was compacted using a roller compactor, following the standard procedure outlined in BS EN 12697-33⁵⁶. The test temperature was maintained at 60 $^\circ\text{C}$, and a total of 10,000 cycles were conducted to assess the performance of the mixes under high-temperature conditions.

To accurately identify the failure mechanisms of the mixes under controlled conditions, the test was conducted to closely simulate field conditions as much as possible. At a lab temperature of 20 $^\circ\text{C}$, these slabs were held in their molds for 1 day. They were then allowed to cure for an additional day at 40 $^\circ\text{C}$, followed by 21 days at lab temperatures, during which a consistent mass was attained according to the procedure of Thanaya¹³.

Low-temperature cracking susceptibility

Utilizing a universal testing machine type (H25KS), a three-point bending test was conducted to evaluate the low-temperature properties of the asphalt mix in accordance with BS EN 12697-44⁵⁷. The test specimens for semi-circular bending (SCB) were first created from slab specimens. After that, the H25KS universal testing apparatus was used to assess how well mixed specimens could withstand cracking at low temperatures. From compacted slabs, several cylindrical specimens with dimensions of 150 mm in diameter and 50 mm in depth were extruded.

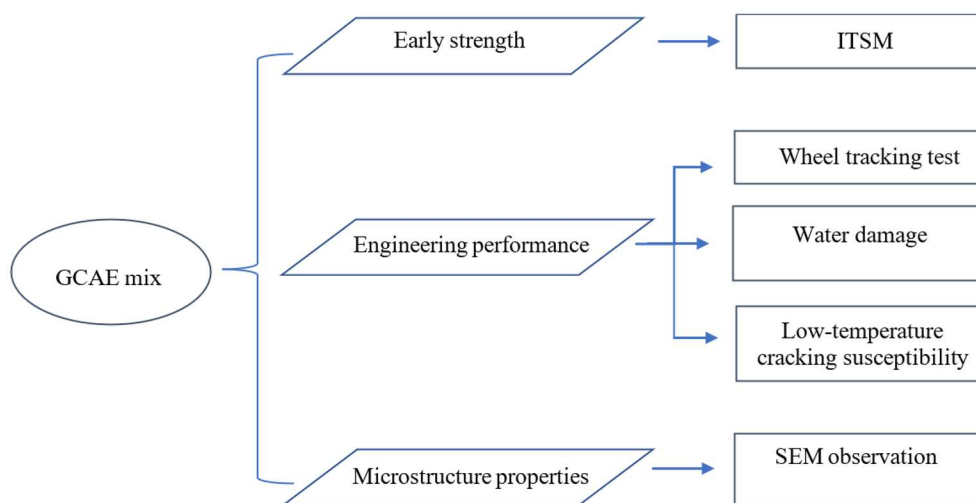


Figure 5. Experimental plans.

The loading speed was 50 mm/min, and the temperature was set at 5 °C. The bending strength was determined based on the three-point bending test to assess the mixtures' sensitivity to fracture at low temperatures⁵⁸. To assess the mixes' susceptibility to low-temperature cracking, the average of three replicates was recorded.

Water sensitivity test

Moisture has a significant impact on the adhesion between the binder and aggregates in asphalt mixtures, leading to crack formation and surface course weakening⁵⁹. To evaluate the durability of the mixtures, the water sensitivity test was conducted in accordance with the British Standard EN 12697-12⁶⁰. The test aimed to assess the resistance of the mixtures to the effects of water. Additionally, the stiffness modulus ratio (SMR), was determined as a measure of the mixtures' resistance to moisture-induced damage.

The cylindrical samples were manufactured and separated into dry and wet sets. One of the sets was submerged in water heated to a conditioning temperature of 40 °C after being wet. The water level was 25 mm over the top surface of the wet group specimens, which were placed in a water bath at 20 °C for 4 days. They spent 10 min at a pressure of 6.7 kPa inside a vacuum container that was kept at lab temperature. They were held under water for a further 30 min when air pressure was progressively introduced into the vacuum container.

Afterwards, the specimens were immersed in a water bath at a temperature of 40 °C for a duration of 72 h. Following the completion of this water immersion period, the dried samples were placed on a flat surface after undergoing the preparation and compaction phases. Following the conditioning procedures, each group's ITSM and SMR were identified.

$$\text{SMR} = (\text{ITSM}_{\text{wet}} / \text{ITSM}_{\text{dry}}) \times 100$$

where SMR: The stiffness modulus ratio. ITSM_{wet} : The indirect tensile stiffness modulus for wet samples. ITSM_{dry} : The indirect tensile stiffness modulus for dry samples. The average of three replicates was recorded to evaluate the water sensitivity of the mixes.

Microstructures test

SEM images were obtained from small dried samples extracted from fully cured paste specimens after a 28-day curing period. These images were used to analyze the microscopic morphology and pore structure of the hydrated product. A "Quanta 200" scanning electron microscope with a working distance of 13 mm and an accelerating voltage of 10 keV was utilized to capture the images at various magnifications.

Results and discussion

ITSM results

It was reported that the practical applications of the CAEM mixes in the need for speedy open traffic can be directly impacted by its early-age strength⁵⁸. In order to acquire a thorough understanding of the CAEM mixture's early-age strength, ITSM was used.

Previous studies have indicated that the optimal combination of GGBFS and CCR in CAEMs is 4% and 2% of the total aggregate mass, respectively⁵¹. The use of a novel cementitious binary blended filler, consisting of GGBFS and CCR, has shown significant effectiveness in enhancing the properties of CAEMs. CCR, with its high alkalinity (pH = 13.1), serves as the activating medium for GGBFS, which acts as a latent hydraulic material. Subsequently, the pre-wetting water is replaced with a waste alkaline $\text{Ca}(\text{OH})_2$ solution to produce a geopolymer cold asphalt emulsion mixture (GCAE). It is worth noting that altering the pH of emulsions can result in their destabilization⁶¹. After a three-day curing period, the GCAE exhibited a maximum stiffness modulus of 2465 MPa, representing a 13-fold improvement compared to the TLF mix, which measured 1678 MPa when incorporating 4% GGBFS + 2% CCR.

Figures 6 and 7 illustrate the progression of the ITSM test results for different mixtures, including TLF, 4GGBFS2CCR, GCAE, and the reference hot mixes, at various curing durations (3, 7, 14, 28, and 56 days). Notably, the ITSM of the GCAE mix exhibited significant improvements across all curing timeframes, surpassing the ITSM of the conventional HMA (100/150 pen) within just 3 days of standard curing.

Remarkably, the ITSM results for these mixes exceeded those of HMA, typically used on heavily trafficked roads, within a mere 3 days. By the 7th day, the GCAE mix demonstrated more than double the performance of HMA 100/150. After 28 days of normal curing, the GCAE mixture exhibited over 110% of the ITSM exhibited by the hard HMA (40/60 pen). This remarkable early-age strength of GCAE can be attributed to the addition of the waste alkaline $\text{Ca}(\text{OH})_2$ solution. The combination of the waste $\text{Ca}(\text{OH})_2$ solution and CCR played a crucial role in activating the latent hydraulic material, GGBFS, resulting in this significant enhancement of ITSM. The hydration products formed as a result of this activation process penetrate the binder bond and disperse throughout it, further strengthening the binder⁶². Furthermore, the elevated pH of the hydration medium aided in the dissolution and disintegration of the glassy phase of the pozzolanic material. Moreover, due to their alkaline nature, the waste alkaline $\text{Ca}(\text{OH})_2$ solution and CCR expedited the breakdown of the cationic bitumen emulsion.

On the other hand, the TLF mix showed inferior performance at all curing ages. The strength development of CAEM primarily relies on two factors: the removal of trapped water and the setting of the bitumen emulsion to its original base bitumen state. Such TLF mix initially showed low strength and gradually acquired some strength with time due to the rising rate of water evaporation. However, compared to the two categories of HMA, its performance is still lacking. It was reported that the early-age strength of the CMA mix can directly affect its practical applications in the requirement of rapid open traffic⁵⁸. It was worth mentioning that the bulk density of the TLF, 4GGBFS2CCR, GCAE, HMA 100/150, and HMA 40/60 were (2.163, 2.175, 2.189, 2.325, and 2.316) g/

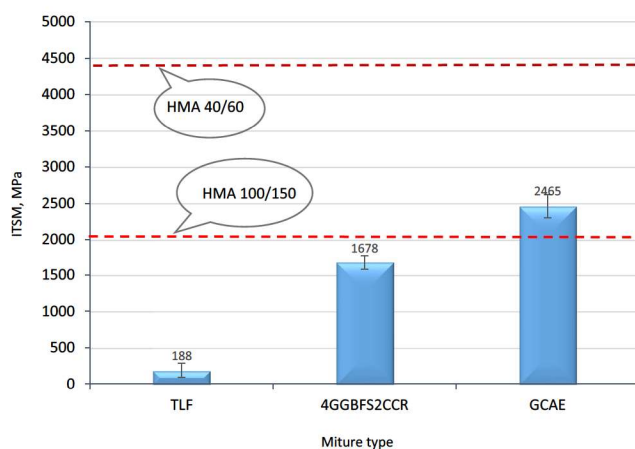


Figure 6. ITSM after 3 curing days.

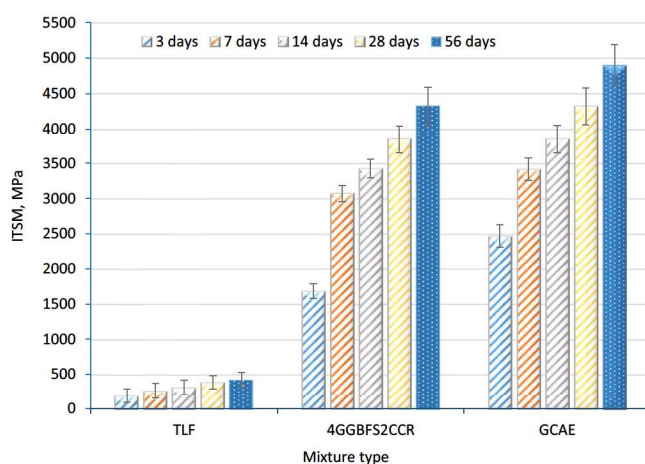


Figure 7. ITSM after 3, 7, 14, 28 and 56 curing days.

cm³, respectively. However, the proximity of density of above cold mixes has a limited effect on their mechanical and durability properties, while the constitutions of the mixes control these properties.

Wheel tracking test results

The rut depths of each mixture combination were calculated using the wheel tracker test. The rut depth in various mixes reached after 10,000 cycles is shown in Fig. 8 below. The control mix (TLF) had a depth of around 9 mm, which was reduced to 2.4 mm by the addition of 4GGBFS2CCR, and further dropped to 1.7 mm by the addition of the waste alkaline Ca(OH)₂ solution to the mixtures. Subsequently, by the addition of the waste alkaline Ca(OH)₂ solution to the filler made from 4GGBFS2CCR, there was a drastic decrease of around 40% in the rut depth in comparison to the 4GGBFS2CCR mix. This shows that the mix had better resistance to rutting susceptibility when the alkaline solution was added.

The reason for this is the improved hydration products. This improves the bonding characteristics of the internal microstructure bonding agent that binds the fine and coarse aggregates. In addition, asphalt emulsion demulsification was sped up by the 4GGBFS2CCR filler. In the meanwhile, the water in the CAEM might promote the hydration process, thus consuming the excess water that normally exists in conventional CAEM, consequently improving the stiffness and rutting resistance of these mixtures^{63,64}.

Furthermore, the replacement of pre-wetting water with the waste alkaline Ca(OH)₂ solution further increased the hydration process. As a result, hydration products as well as asphalt films may be joined to create a network structure that would offer exceptional deformation resistance. Similar behaviour was also reported by Lu et al.⁵⁸.

Low-temperature cracking susceptibility results

The fracture toughness values are presented in Fig. 9. As suggested in this figure, the TLF mix had the lowest bending fracture toughness value. This might be caused by the TLF mix's low ITSM, which has a significant impact on the fracture propagation mechanism. When 4GGBFS2CCR was used, the fracture toughness values

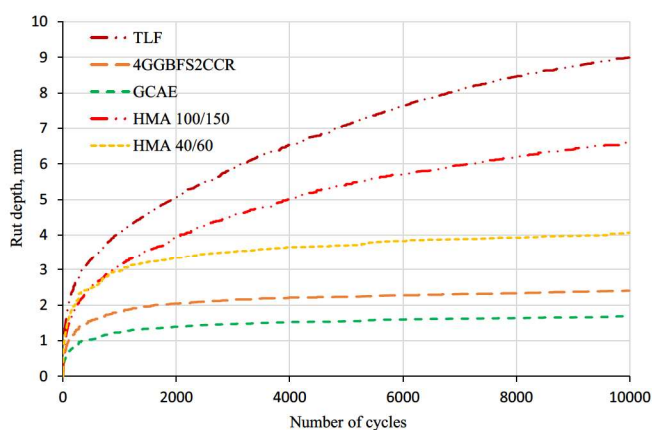


Figure 8. Wheel track results.

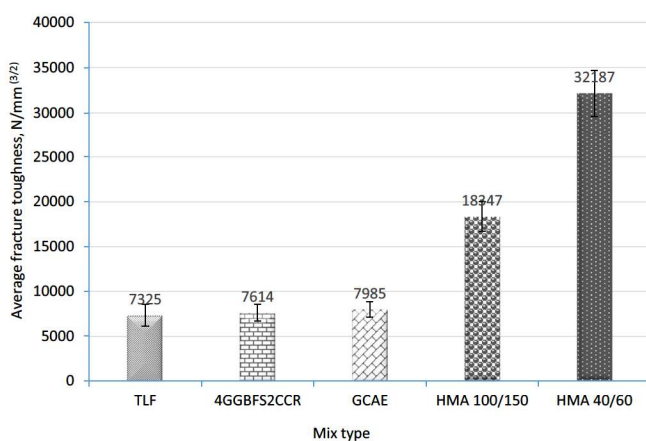


Figure 9. Fracture toughness for the mixes.

of the mixes increased to 7614 N/mm^{2/3}, meaning an increment of approximately 4%. This is expected because both GGBFS and CCR increased the stiffness of the mixtures. Additionally, the fracture toughness values could further be increased to about 7985 N/mm^{2/3} for GCAE, which is about 9% higher than that of the TLF mix. This can be attributed to the effect of the increase in ITSM. However, all these mixes have less fracture toughness in comparison to both HMA (100/150 pen) and HMA (40/60 pen).

Water damage results

The ITSM and SMR values of mixes containing the employed ingredients are shown in Fig. 10. It is evident that both the ITSM and SMR values showed an increase when 4GGBFS2CCR (4% GGBFS + 2% CCR) were utilized. Furthermore, the incorporation of the waste alkaline Ca(OH)₂ solution resulted in the highest values for both ITSM and SMR.

Its SMR value for the TLF mix was only 75%. The cementitious filler 4GGBFS2CCR substantially raised the SMR value to 101%. Similar to this, the waste alkaline Ca(OH)₂ solution that was integrated showed a higher SMR value of 103%. Other reports have supported similar outcomes⁵⁸. This was mostly due to the use of GGBFS and CCR that were activated by the waste alkaline Ca(OH)₂ solution, which produced many hydration products that increased the strength and stiffness of the GCAE. These findings align with the research conducted by Tian et al.⁶⁵, which demonstrated improved water susceptibility when incorporating a high content of cement in CAEMs. The advantage of introducing GGBFS, CCR, and the waste alkaline Ca(OH)₂ solution increased the formation of hydration products and enhanced water susceptibility.

SEM observation

SEM analysis was conducted on the samples to confirm the development of cementitious products in the 4GGBFS-2CCR geopolymer over time. The formation of a dense cementation matrix can be attributed to the chemical reaction between SiO₂, Al₂O₃, and MgO (present in GGBFS) and CaO and SiO₂ (present in CCR), which effectively binds the particles together. The SEM images reveal the presence of a more continuous matrix with a

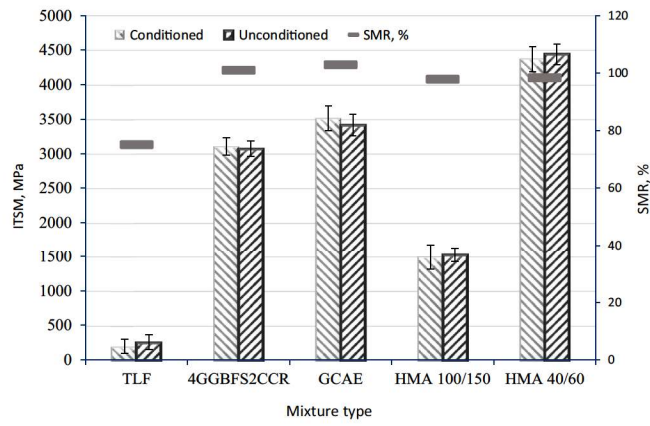


Figure 10. Water damage resistance results.

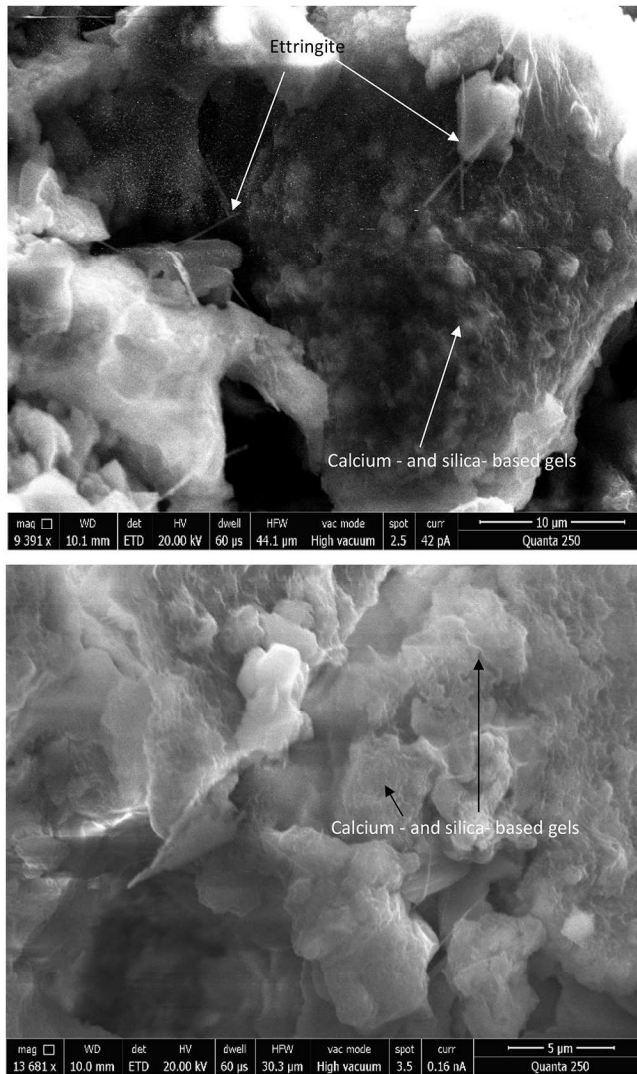


Figure 11. The morphology details of the microstructures of GCAE at 28 days.

denser structure. Notably, Fig. 11a and b indicate the absence of a residual shell formed by large-sized GGBFS and CCR particles, indicating their erosion by the alkaline solution.

The SEM analysis reveals that the pozzolanic reactions, containing calcium- and silica- based gels and needles fill the pore structure and contribute to the increased density of the mixture. The microstructure appears dense, with the presence of various cement hydrates and no visible voids. As a result, the paste sample exhibits a dense microstructure and higher strength. Furthermore, upon closer inspection, the surface of the hardened paste specimen appears smooth without any uneven protrusions. The formation of calcium- and silica- based gels and needles contributes to the densification of the matrix. According to Shi and Day⁶⁶, the initial pH of the activating medium plays a crucial role in the alkali-activated slag process, influencing the early reaction products' formation and the dissolution of slag. Consequently, the performance properties of GCAE are enhanced.

The dense structure of the calcium- and silica- based gels and needles and asphalt films contributes to the formation of a network structure, leading to improved strength in GCAE. The predominant presence of the calcium- and silica- based gels phase contributes to the regular and compact microstructure. Additionally, under further magnification, needle-like crystals can be observed filling the voids left by water evaporation. The exceptional early-age strength performance of GCAE mixes can be attributed to the evident densification of the microstructure. These findings align with previous studies conducted by Lu et al.⁵⁸ and Dulaimi et al.⁴⁶.

Conclusions

Based on the research findings regarding the mechanical properties, work performance, and hydration characteristics of the geopolymer cold asphalt emulsion mixture (GCAE) incorporating waste alkaline $\text{Ca}(\text{OH})_2$ solution, ground granulated blast-furnace slag (GGBFS), and calcium carbide residue (CCR), the following conclusions can be drawn:

1. Because of the considerable curing period required for CAEM to acquire full strength after paving, the use of such mixes using TLF as structural layers is not feasible.
2. The waste alkaline $\text{Ca}(\text{OH})_2$ solution is favorable to enhance the mechanical properties of GCAE. The substitution of such material causes the increase of hydration product content. Furthermore, such a solution can improve the performance properties of GCAE.
3. The GCAE mixture exhibits enhanced early-age strength, as indicated by an increased stiffness modulus. It outperforms traditional hot mix asphalt (HMA) within a short curing period, demonstrating its potential for high-performance applications. The ITSM increased due to the addition of waste alkaline $\text{Ca}(\text{OH})_2$ solution along with both GGBFS and CCR fillers. Notably, the ITSM of the GCAE in this study increased by approximately 13 times compared to the traditional LF mix after 3 days of curing. The addition of waste alkaline $\text{Ca}(\text{OH})_2$ solution significantly contributed to outstanding early-age strength.
4. The rut depth was significantly lower compared to the reference TLF mix due to the utilization of waste alkaline $\text{Ca}(\text{OH})_2$ solution, GGBFS, and CCR fillers, resulting in rut depths 5.5 times shallower than the traditional LF mix. Additionally, there was a substantial improvement in rutting resistance, with increases of 2.5 and 4 times compared to traditional HMA 100/150 and HMA 40/60, respectively. This suggests that these waste materials substantially enhance material stiffness while also reducing rut depths at high temperatures. Therefore, it is well-suited for use in road pavements exposed to challenging service conditions, including temperature variations.
5. Early-age GCAE strength was high and rapidly developed in the waste alkaline $\text{Ca}(\text{OH})_2$ solution. After 3 days of curing, the ITSM from such mix reached more than 2465 MPa and was roughly 50% of what it was at 28 days, demonstrating that this design approach may be used to produce GCAE with exceptional early-age strength.
6. The increase in the stiffness modulus ratio (SMR) was also observed when the waste alkaline $\text{Ca}(\text{OH})_2$ solution replaced pre-wetting water in the mixtures, showing higher resistance to moisture. Notably, the SMR value exhibited an approximately 40% increase compared to the traditional LF mix. Furthermore, the SMR increase exceeded 5% when compared to hot mix asphalt (HMA). This suggests that the waste alkaline $\text{Ca}(\text{OH})_2$ solution, in combination with GGBFS and CCR fillers, added to the mixtures, provided both high stiffness and strong bonding.
7. The asphalt emulsion was demulsified with the use of the waste alkaline $\text{Ca}(\text{OH})_2$ solution, GGBFS, and CCR fillers, resulting in a much higher amount of hydration products and a regular, compact microstructure. The excellent stiffness has, nevertheless, resulted in a minor improvement in the cracking susceptibility.
8. The utilization of GGBFS and CCR as fillers in the GCAE mixture contributes to the formation of a dense cementation matrix. This matrix, formed by the reaction between various compounds in GGBFS and CCR, improves the binding between particles and results in a stronger and more durable pavement structure.

These findings suggest that the incorporation of waste alkaline $\text{Ca}(\text{OH})_2$ solution, GGBFS, and CCR in the geopolymer cold asphalt emulsion mixture offers a promising solution for achieving high-performance and sustainable asphalt pavements. The following steps will be implemented at the construction site, and we recommend the use of GCAE mix to enhance the initial road performance. Further research and development in this area can lead to the utilization of industrial by-products and the production of more durable and environmentally friendly road materials.

Limitations and novelty of research

While this study has provided valuable insights and promising results, it is crucial to recognize its limitations. It's worth noting that certain tests within this research had relatively short time frames. A more extended evaluation of performance and durability in the long term may uncover further insights and potential challenges not addressed in this study. Furthermore, the experiments were carried out within controlled laboratory settings, which may not fully account for real-world conditions, including traffic loads and environmental factors, which can introduce additional complexities.

In spite of its limitations, this research makes several noteworthy contributions. The incorporation of waste alkaline Ca(OH)₂ solution, combined with GGBFS and CCR fillers in asphalt mixtures, introduces an innovative approach to enhancing sustainability in road construction. The substantial enhancements in stiffness, rutting resistance, and bonding observed in this study underscore the potential for these waste materials to elevate asphalt mixture performance. Moreover, the research underscores the efficacy of the waste alkaline Ca(OH)₂ solution in enhancing moisture resistance, a critical factor in road pavement durability.

Received: 2 September 2023; Accepted: 10 October 2023

Published online: 13 October 2023

References

- Huang, B., Li, G., Vukosavljevic, D., Shu, X. & Egan, B. K. Laboratory investigation of mixing hot-mix asphalt with reclaimed asphalt pavement. *Transp. Res. Rec.* **1929**(1), 37–45 (2005).
- Ling, C., Hanz, A. & Bahia, H. Measuring moisture susceptibility of Cold Mix Asphalt with a modified boiling test based on digital imaging. *Constr. Build. Mater.* **105**, 391–399 (2016).
- Diab, A., Sangiorgi, C., Ghabchi, R., Zaman, M., Wahaballa, A. M., Lee, Y. H., Chou, N. N., He, J., Qian, G. & Zhu, J. *Warm Mix Asphalt (WMA) Technologies: Benefits and Drawbacks—A Literature Review*. Functional Pavement Design (October 14, 2016), 1145–1154 (2016).
- Caro, S., Beltrán, D. P., Alvarez, A. E. & Estakhri, C. Analysis of moisture damage susceptibility of warm mix asphalt (WMA) mixtures based on dynamic mechanical analyzer (DMA) testing and a fracture mechanics model. *Constr. Build. Mater.* **35**, 460–467 (2012).
- Xu, S., Xiao, F., Amirhanian, S. & Singh, D. Moisture characteristics of mixtures with warm mix asphalt technologies—A review. *Constr. Build. Mater.* **142**, 148–161 (2017).
- Al Nageim, H., Dulaimi, A., Ruddock, F. & Seton, L. Development of a new cementitious filler for use in fast-curing cold binder course in pavement application. In *The 38th International Conference on Cement Microscopy* 167–180 (2016).
- Lu, S.-M., Lu, C., Tseng, K.-T., Chen, F. & Chen, C.-L. Energy-saving potential of the industrial sector of Taiwan. *Renew. Sustain. Energy Rev.* **21**, 674–683 (2013).
- Ge, Z., Li, H., Han, Z. & Zhang, Q. Properties of cold mix asphalt mixtures with reclaimed granular aggregate from crushed PCC pavement. *Constr. Build. Mater.* **77**, 404–408 (2015).
- Dash, S. S. & Panda, M. Influence of mix parameters on design of cold bituminous mix. *Constr. Build. Mater.* **191**, 376–385 (2018).
- Thanaya, I. N. A., Zoorob, S. E. & Forth, J. P. A laboratory study on cold-mix, cold-lay emulsion mixtures. *Proc. Inst. Civ. Eng. Transp.* **162**(1), 47–55 (2009).
- Leech, D. *Cold Asphalt Materials for Use in the Structural Layers of Roads*. Project Report 75, Transport Research Laboratory (1994).
- Read, J. & Whiteoak, D. *The Shell Bitumen Handbook—Fifth Edition* (2003).
- Thanaya, I. N. A. *Improving the Performance of Cold Bituminous Emulsion Mixtures Incorporating Waste Materials* (University of Leeds, 2003).
- Dulaimi, A., Nageim, H. A., Ruddock, F. & Seton, L. Laboratory studies to examine the properties of a novel cold-asphalt concrete binder course mixture containing binary blended cementitious filler. *J. Mater. Civ. Eng.* **29**(9), 04017139 (2017).
- Shanbara, H. K., Ruddock, F. & Atherton, W. A laboratory study of high-performance cold mix asphalt mixtures reinforced with natural and synthetic fibres. *Constr. Build. Mater.* **172**, 166–175 (2018).
- Fang, X., Garcia, A., Winnefeld, F., Partl, M. N. & Lura, P. Impact of rapid-hardening cements on mechanical properties of cement bitumen emulsion asphalt. *Mater. Struct.* **49**, 487 (2016).
- Wang, Z. & Sha, A. Micro hardness of interface between cement asphalt emulsion mastics and aggregates. *Mater. Struct.* **43**(4), 453–461 (2010).
- Oruc, S., Celik, F. & Akpınar, V. Effect of cement on emulsified asphalt mixtures. *J. Mater. Eng. Perform.* **16**(5), 578–583 (2007).
- Shanbara, H. K., Dulaimi, A. & Al-Mansoori, T. Studying the mechanical properties of improved cold emulsified asphalt mixtures containing cement and lime. *IOP Conf. Ser. Mater. Sci. Eng.* **1090**(1), 012006 (2021).
- Wang, F., Liu, Y. & Hu, S. Effect of early cement hydration on the chemical stability of asphalt emulsion. *Constr. Build. Mater.* **42**, 146–151 (2013).
- Xie, T. & Ozbakkaloglu, T. Influence of coal ash properties on compressive behaviour of FA- and BA-based GPC. *Mag. Concr. Res.* **67**(24), 1301–1314 (2015).
- Chindaprasirt, P., Chareerat, T. & Sirivivatnanon, V. Workability and strength of coarse high calcium fly ash geopolymer. *Cem. Concr. Compos.* **29**(3), 224–229 (2007).
- Shanbara, H. K. *et al.* The future of eco-friendly cold mix asphalt. *Renew. Sustain. Energy Rev.* **149**, 111318 (2021).
- Dulaimi, A., Al Nageim, H., Ruddock, F. & Seton, L. Assessment the performance of cold bituminous emulsion mixtures with cement and supplementary cementitious material for binder course mixture. In *The 38th International Conference on Cement Microscopy*, 283–296 (2016).
- Sarıdemir, M., Topçu, İB., Özcan, F. & Severcan, M. H. Prediction of long-term effects of GGBFS on compressive strength of concrete by artificial neural networks and fuzzy logic. *Constr. Build. Mater.* **23**(3), 1279–1286 (2009).
- Ellis, C., Zhao, B., Barnes, J. & Jones, N. Properties of GGBS-bitumen emulsion systems with recycled aggregates. *Road Mater. Pavement Des.* **5**(3), 373–383 (2004).
- Yadav, R. K. & Choudhary, P. Marshall properties of SDBC using emulsion based cold mix technology. *Int. J. Res. Appl. Sci. Eng. Technol.* ISSN, 2321–9653.
- Nassar, A. I., Mohammed, M. K., Thom, N. & Parry, T. Characterisation of high-performance cold bitumen emulsion mixtures for surface courses. *Int. J. Pavement Eng.* **19**(6), 509–518 (2018).
- Bijen, J. Benefits of slag and fly ash. *Constr. Build. Mater.* **10**(5), 309–314 (1996).
- Özbay, E., Erdemir, M. & Durmuş, H. I. Utilization and efficiency of ground granulated blast furnace slag on concrete properties—A review. *Constr. Build. Mater.* **105**, 423–434 (2016).
- Wang, Q., Sun, S.-K., Wang, Z.-M. & Lyu, X.-J. Physical properties, hydration mechanism, and leaching evaluation of the Portland cement prepared from carbide residue. *J. Clean. Prod.* **366**, 132777 (2022).

32. Sadique, M. & Coakley, E. The influence of physico-chemical properties of fly ash and CKD on strength generation of high-volume fly ash concrete. *Adv. Cem. Res.* **28**(9), 595–605 (2016).
33. Hanjitsuwan, S., Phoo-ngernkham, T. & Damrongwiriyanupap, N. Comparative study using Portland cement and calcium carbide residue as a promoter in bottom ash geopolymer mortar. *Constr. Build. Mater.* **133**, 128–134 (2017).
34. Pang, Y., Zhu, X., Yang, M. & Yu, J. Tailoring rheological–strength–ductility properties of self-cleaning geopolymer composites with asphalt emulsion. *Constr. Build. Mater.* **308**, 124997 (2021).
35. Jiang, X. *et al.* A comparative study on geopolymers synthesized by different classes of fly ash after exposure to elevated temperatures. *J. Clean. Prod.* **270**, 122500 (2020).
36. Jiang, X. *et al.* A laboratory investigation of steel to fly ash-based geopolymer paste bonding behavior after exposure to elevated temperatures. *Constr. Build. Mater.* **254**, 119267 (2020).
37. Milad, A., Ali, A. S. B., Babalghaith, A. M., Memon, Z. A., Mashaan, N. S., Arafa, S. & Md. Yusoff, N. I. Utilisation of waste-based geopolymer in asphalt pavement modification and construction—A review. *Sustainability* **13**(6) (2021).
38. Hoy, M., Horpibulsuk, S. & Arulrajah, A. Strength development of recycled asphalt pavement—Fly ash geopolymer as a road construction material. *Constr. Build. Mater.* **117**, 209–219 (2016).
39. Wongkvanklom, A., Posi, P., Kampala, A., Kaewngao, T. & Chindaprasirt, P. Beneficial utilization of recycled asphaltic concrete aggregate in high calcium fly ash geopolymer concrete. *Case Stud. Const. Mater.* **15**, e00615 (2021).
40. Meng, Y., Lei, J., Zhang, R., Yang, X., Zhao, Q., Liao, Y. & Hu, Y. Effect of geopolymer as an additive on the mechanical performance of asphalt. *Road Mater. Pavement Des.* 1468–0629 (2021).
41. Tang, N. *et al.* Geopolymer as an additive of warm mix asphalt: Preparation and properties. *J. Clean. Prod.* **192**, 906–915 (2018).
42. Suwan, T. *et al.* Properties and microstructures of crushed rock based-alkaline activated material for roadway applications. *Materials* <https://doi.org/10.3390/ma15093181> (2022).
43. Bualuang, T. *et al.* Non-OPC binder based on a hybrid material concept for sustainable road base construction towards a low-carbon society. *J. Mater. Res. Technol.* **14**, 374–391 (2021).
44. European Committee for Standardization, *BS EN 933-1:2012: Tests for Geometrical Properties of Aggregates-Part 1: Determination of Particle Size Distribution-Sieving Method* (British Standards Institution, 2012).
45. Shanbara, H. K., Ruddock, F. & Atherton, W. Predicting the rutting behaviour of natural fibre-reinforced cold mix asphalt using the finite element method. *Constr. Build. Mater.* **167**, 907–917 (2018).
46. Dulaimi, A., Al Nageim, H., Ruddock, F. & Seton, L. High performance cold asphalt concrete mixture for binder course using alkali-activated binary blended cementitious filler. *Constr. Build. Mater.* **141**, 160–170 (2017).
47. Ajala, E. O., Ajala, M. A., Ajao, A. O., Saka, H. B. & Oladipo, A. C. *Calcium-Carbide Residue: A Precursor for the Synthesis of CaO-Al₂O₃-SiO₂-CaSO₄ Solid Acid Catalyst for Biodiesel Production Using Waste Lard* (2020).
48. Market Research Store, Acetylene gas market for chemical production, welding & cutting and other applications: Global industry perspective, comprehensive analysis and forecast, 2014–2020. *Market Res. Store Rep.* 110 (2015).
49. Hanjitsuwan, S., Phoo-ngernkham, T., Li, L.-Y., Damrongwiriyanupap, N. & Chindaprasirt, P. Strength development and durability of alkali-activated fly ash mortar with calcium carbide residue as additive. *Constr. Build. Mater.* **162**, 714–723 (2018).
50. Chaunsali, P. & Peethampanan, S. Evolution of strength, microstructure and mineralogical composition of a CKD–GGBFS binder. *Cem. Concr. Res.* **41**(2), 197–208 (2011).
51. Dulaimi, A., Shanbara, H. K. & Al-Rifaie, A. The mechanical evaluation of cold asphalt emulsion mixtures using a new cementitious material comprising ground-granulated blast-furnace slag and a calcium carbide residue. *Constr. Build. Mater.* **250**, 118808 (2020).
52. Dulaimi, A., Al-Busaltan, S. & Sadique, M. The development of a novel, microwave assisted, half-warm mixed asphalt. *Constr. Build. Mater.* **301**, 124043 (2021).
53. Asphalt Institute, *Asphalt Cold Mix Manual, Manual Series no. 14(MS-14)* 3rd edn, 40512–4052 (1989).
54. European Committee for Standardization, *BS EN 12697: Part 26. Bituminous Mixtures-Test Methods for Hot Mix Asphalt—Stiffness* (British Standards Institution, 2012).
55. European Committee for Standardization, *BS EN 12697: Part 22. Bituminous Mixtures—Test Methods for Hot Mix Asphalt—Wheel Tracking Test Methods for Hot Mix Asphalt* (British Standards Institution, 2003).
56. European Committee for Standardization, *BS EN 12697: Part 33. Bituminous Mixtures—Test Methods for Hot Mix Asphalt—Specimen Prepared by Roller Compactor* (British Standards Institution, 2003).
57. European Committee for Standardization, *BS EN 12697: Part 44. Bituminous Mixtures-Test Methods for Hot Mix Asphalt-Crack Propagation by Semi-Circular Bending Test* (British Standards Institution, 2010).
58. Lu, D., Wang, Y., Leng, Z. & Zhong, J. Influence of ternary blended cementitious fillers in a cold mix asphalt mixture. *J. Clean. Prod.* **318**, 128421 (2021).
59. Guo, H. *et al.* Effects of dolomite powder on properties of environment-friendly cement asphalt emulsion composites. *J. Clean. Prod.* **369**, 133321 (2022).
60. European Committee for Standardization, *BS EN 12697: Part 12. Bituminous Mixtures-Test Methods for Hot Mix Asphalt-Determination of the Water Sensitivity of Bituminous Specimens* (British Standard Institution, 2008).
61. Ronald, M. & Luis, F. P. Asphalt emulsions formulation: State-of-the-art and dependency of formulation on emulsions properties. *Constr. Build. Mater.* **123**, 162–173 (2016).
62. Du, S. Effect of curing conditions on properties of cement asphalt emulsion mixture. *Constr. Build. Mater.* **164**, 84–93 (2018).
63. Bualuang, T. *et al.* Influence of asphalt emulsion inclusion on fly ash/hydrated lime alkali-activated material. *Materials* <https://doi.org/10.3390/ma14227017> (2021).
64. Bualuang, T., Jitsangiam, P., Rattanasak, U., Suwan, T., Aryupong, C. and Nikraz, H. Characterisation of road base materials treated by hybrid alkali-activated binders and cationic asphalt emulsions. *Int. J. Pavement Eng.* 1–10.
65. Tian, Y. *et al.* Effects of cement contents on the performance of cement asphalt emulsion mixtures with rapidly developed early-age strength. *Constr. Build. Mater.* **244**, 118365 (2020).
66. Shi, C. & Day, R. L. A calorimetric study of early hydration of alkali-slag cements. *Cem. Concr. Res.* **25**(6), 1333–1346 (1995).

Acknowledgements

The financial support of University of Warith Al-Anbiyaa in Iraq is gratefully acknowledged.

Author contributions

A.D.: conceptualization, methodology, formal analysis, investigation, resources, data curation, writing (original draft), supervision, project administration, funding acquisition. S.A-B.: conceptualization, methodology, data curation, formal analysis, writing (original draft), project administration. M.A.O.M.: methodology, formal analysis, investigation, resources. D.L.: methodology, formal analysis, investigation, resources. Y.O.Ö.: methodology, validation, investigation, resources. R.P.J.: methodology, validation, investigation, resources. A.A.: methodology, validation, investigation, resources, funding acquisition, project administration. All authors reviewed the manuscript.

Funding

Open access funding provided by University of Gävle.

Competing interests

The authors declare no competing interests.

Additional information

Correspondence and requests for materials should be addressed to A.D. or A.A.

Reprints and permissions information is available at www.nature.com/reprints.

Publisher's note Springer Nature remains neutral with regard to jurisdictional claims in published maps and institutional affiliations.



Open Access This article is licensed under a Creative Commons Attribution 4.0 International License, which permits use, sharing, adaptation, distribution and reproduction in any medium or format, as long as you give appropriate credit to the original author(s) and the source, provide a link to the Creative Commons licence, and indicate if changes were made. The images or other third party material in this article are included in the article's Creative Commons licence, unless indicated otherwise in a credit line to the material. If material is not included in the article's Creative Commons licence and your intended use is not permitted by statutory regulation or exceeds the permitted use, you will need to obtain permission directly from the copyright holder. To view a copy of this licence, visit <http://creativecommons.org/licenses/by/4.0/>.

© The Author(s) 2023